

Specific Cu²⁺-induced J-aggregation and Hg²⁺-induced fluorescence enhancement based on BODIPY

Hua Lu, Zhaoli Xue, John Mack, Zhen Shen*, Xiaozeng You and Nagao Kobayashi*.

Electronic Supplementary Information

I. Experimental section

I.1 Synthesis and characterisation.....	S2–S3
I.2 X-ray structure determination.....	S3
I.3 Procedures of metal ion sensing.....	S4
I.4 DFT calculations.....	S4

II. Supplementary Figure

Figure S1 (Molecular packing in the crystal structure of 1)	S5
Figure S2 (Colour changes in solutions of 1 upon addition of different metals)	S6
Figure S3 (Reversibility of J-aggregate formation of [(Cu ²⁺)(1) ₂])	S6
Figure S4 (Frontier π -MOs and TD-DFT spectra of 1 and a model complex)	S7
Figure S5 (Frontier π -MOs and TD-DFT spectra of 1 and a model complex)	S8
Figure S6 (Model diagram for [(Cu ²⁺)(1) ₂] J-aggregate formation of)	S9

III. References

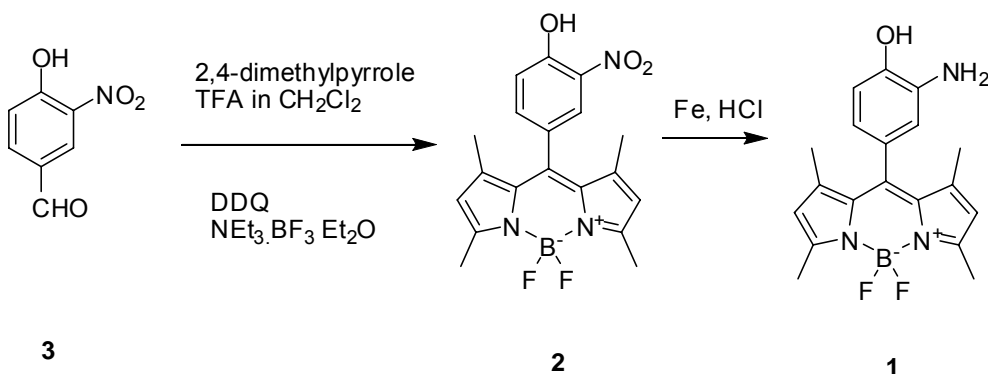
IV. ¹H NMR spectra

S11–S12

I. Experimental Section

All reagents were obtained from commercial suppliers and used without further purification unless otherwise indicated. Air- and moisture-sensitive reactions were carried out under a nitrogen atmosphere using oven-dried glassware. Dichloromethane was distilled over calcium hydride. Triethylamine was obtained by simple distillation. Elemental analyses for C, H and N were performed on a Perkin-Elmer 240C elemental analyzer. ^1H NMR spectra were recorded on a Bruker DRX500 spectrometer with the residual solvent peaks used as the reference signals. Mass spectra were measured with a Bruker Daltonics Autoflex IITM MALDI TOF spectrometer. Luminescence spectra were measured on an Aminco Bowman 2 Luminescence spectrophotometer. The fluorescence quantum yield was calculated using Rhodamine 6G ($\phi_F = 0.88$ in EtOH) as a reference.^{S1}

I.1 Synthesis routes and characteristic data



Scheme S1. The synthetic route for BDP compounds **1** and **2**

Synthesis of 8-(3-nitro-4-hydroxyphenyl)-4,4-difluoro-1,3,5,7-tetramethyl 4-bora-3a,4a-diaza-s-indacene (**2**)^{S2}

2,4-dimethylpyrrole (380mg, 4mmol) and 3-nitro-4-hydroxybenzaldehyde (334mg, 2mmol) were dissolved in dry CH_2Cl_2 (150mL) under nitrogen. One drop of trifluoroacetic acid (TFA) was added, and the solution was stirred overnight at ambient temperature in the dark until TLC indicated complete consumption of the aldehyde. Dichlorodicyanobenzoquinone (DDQ, 442mg, 2mmol) was added, and the mixture was stirred for additional 30 min. The reaction mixture was then treated with triethylamine (3mL) and stirring was continued for a further 5 min. Boron trifluoride etherate (3mL) was added. After stirring for another 40 min, the dark brown solution was washed with water ($3 \times 20\text{mL}$) and brine (30mL), dried over anhydrous magnesium sulphate and concentrated at reduced pressure. **2** (150 mg, 19% yield) was

purified by silica–gel flash column chromatography (silica gel, 10% EtOAc/Petroleum ether) and recrystallisation (mp > 200 °C (CHCl₃/hexane)) yielded red crystals (Found: C, 59.38; H, 4.63; N, 10.93. C₁₉H₁₈N₃O₃BF₂ requires C, 59.25; H, 4.71; N, 10.91); λ_{\max} (CHCl₃)/nm 479 ($\epsilon/\text{dm}^3 \text{ mol}^{-1} \text{ cm}^{-1}$ 14 800) and 507 (61 700); ν_{\max} (KBr pellet)/cm⁻¹ 3447, 2924, 1634, 1548, 1512, 1465, 1415, 1382, 1311, 1192, 1156, 1088 and 937 cm⁻¹; δ_{H} (500 MHz; CDCl₃) 10.73 (1 H, s), 8.13 (1 H, s), 7.55 (1 H, d, *J* = 5 Hz), 7.36 (1 H, d, *J* = 8.5 Hz), 6.05 (2 H, s), 2.586 (6 H, s) and 1.49 (6 H, s); *m/z* (MALDI–TOF) 385.210 [M]⁺.

Synthesis of 8–(3–amino–4–hydroxyphenyl)–4,4–difluoro–1,3,5,7–tetramethyl 4–bora–3a, 4a –diazas–indacene (1)

BODIPY compound **2** (150mg, 0.39mmol) was dissolved in 5 ml of methanol. Fe (300 mg, 5.4 mmol) in 3ml of H₂O was added, the solution was heated to reflux and 2 ml of a 0.6 M hydrochloric acid solution in methanol was then slowly added dropwise. The solution was stirred at reflux for 2 h until TLC monitoring indicated complete consumption of the starting material and was then cooled to room temperature, filtered and concentrated at reduced pressure. **1** (105 mg, yield 75%) was purified by silica–gel flash column chromatography (silica gel, 20% EtOAc/Petroleum ether) and recrystallisation (mp > 200 °C (CHCl₃/hexane)) yields red crystals (Found: C, 64.43; H, 5.62; N, 11.72. C₁₉H₂₀N₃OBF₂ requires C, 64.25; H, 5.68; N, 11.83); λ_{\max} (CHCl₃)/nm 474 ($\epsilon/\text{dm}^3 \text{ mol}^{-1} \text{ cm}^{-1}$ 12 900) and 502 (56 700); ν_{\max} (KBr pellet)/cm⁻¹ 3430, 2923, 1620, 1544, 1507, 1469, 1406, 1382, 1302, 1197, 1158, 1085 and 983; δ_{H} (500 MHz; CDCl₃) 6.84 (1 H, d, *J* = 9 Hz), 6.66 (1 H, s), 6.56 (1 H, d, *J* = 7.5 Hz), 5.99 (2 H, s), 2.56 (6 H, s) and 1.54 (6 H, s); *m/z* (MALDI–TOF) 355.148 [M]⁺, 336.157 [M–F]⁺.

1.2 X–ray structure determination:

A single crystal of compound **1** was selected under a microscope and mounted on a glass fibre. The unit cell parameters and data were collected on a Bruker Smart Apex CCD diffractometer with graphite monochromatised Mo K α radiation (λ = 0.71073 Å) using the ω –2 θ scan mode. The data were corrected for Lorentz and polarisation effects. The structure was solved by direct methods and refined on F^2 by full–matrix least–squares methods using the SHELXTL–2000 program package.^{S3}

1: C₁₉H₂₀BF₂N₃O: A red block–like crystal of the approximate dimensions 0.17 × 0.18 × 0.20 mm³ was measured. Monoclinic, space group *P* 2₁/*c*, *a* = 15.941(4) Å, *b* = 7.638(2) Å, *c* = 18.761(3) Å, β = 126.05(2)°, *V* = 1857.7(9) Å³, *Z* = 4, *F*(000) = 744, ρ = 1.271 Mgm⁻³, $2\theta_{\max}$ = 50°, *R*₁ = 0.0701, *wR*(*F*₂) = 0.2172, GOF = 0.989, residual electron density between 0.378

and $-0.453 \text{ e}\text{\AA}^{-3}$.

CCDC 756287 contains the supplementary crystallographic data for this paper. These data can be obtained free of charge via www.ccdc.cam.ac.uk/conts/retrieving.html (or from the Cambridge Crystallographic Data Centre, 12 Union Road, Cambridge CB2 1EZ, UK; fax: (+44)1223-336-033; E-mail: deposit@ccdc.cam.ac.uk).

I.3 Procedures of metal ion sensing

Stock solutions of the metal ions (100 mM and 10 mM) were prepared in deionised water. A stock solution of **1** (0.5 mM) was prepared in DMSO. The solution of **1** was then diluted to 5 μM with HEPES buffer solution (50 mM KNO_3 , 50 mM HEPES, pH 7.2). During titration experiments, 2 mL solutions of **1** (5 μM , 0.5 μM) were placed in a 1 cm quartz optical cell and Cu^{2+} , Hg^{2+} stock solutions were added gradually with a micropipette. Spectral data were recorded immediately after each addition. In selectivity experiments, the test samples were prepared by adding appropriate amounts of the metal ion stock solution into the 2 mL solution of **1** (5 μM). During fluorescence measurements, the excitation wavelength was 483 nm and emission spectra were collected between 495 – 600nm.

I.4 DFT Calculation

The G03W software package^{S4} was used to carry out a DFT geometry optimisation for **1** and a model complex with no $-\text{NH}_2$ and $-\text{OH}$ groups on the phenyl substituent using the B3LYP functional with 6-31G(d) basis sets. TD-DFT calculations were then carried out using the same approach.

II. Supplementary Figure

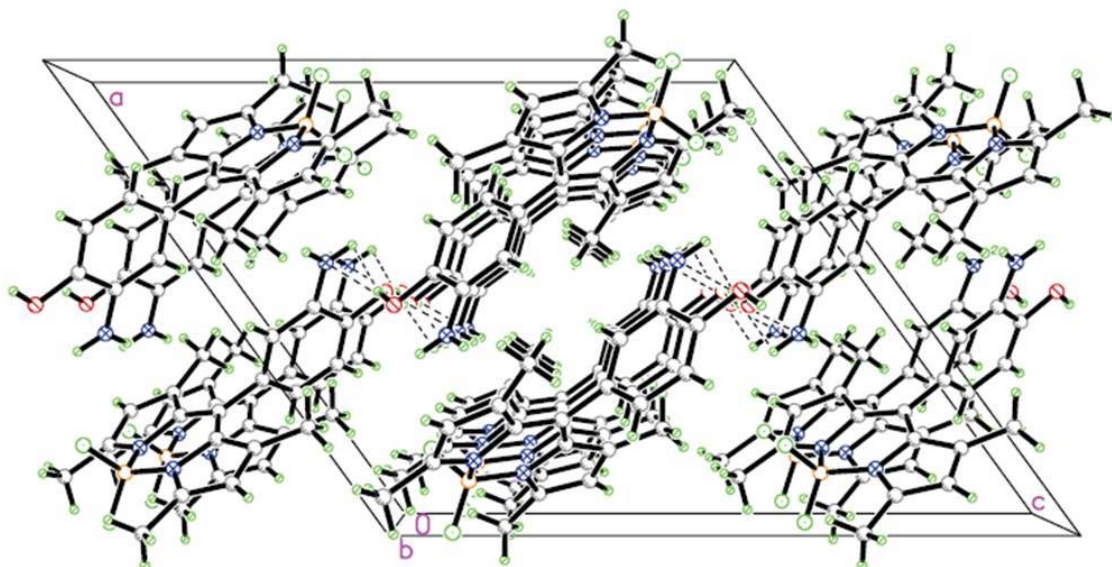


Fig. S1 The molecular packing viewed along the *b*-axis in the crystal structure of 1.

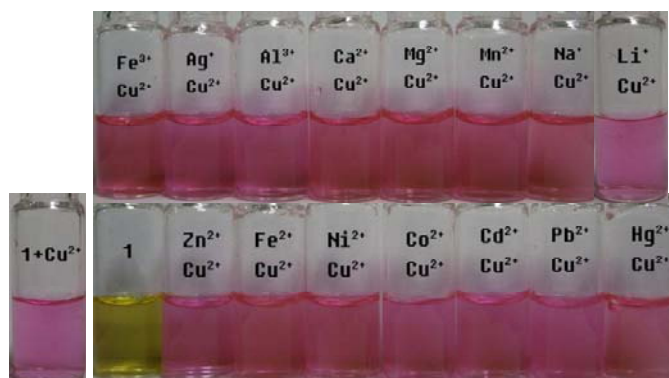


Fig. S2 Colour changes in solutions of **1** (20 μM) upon addition of 100 μM different metal ions and the further addition of 20 μM of Cu^{2+} in DMSO/HEPES buffer solution.

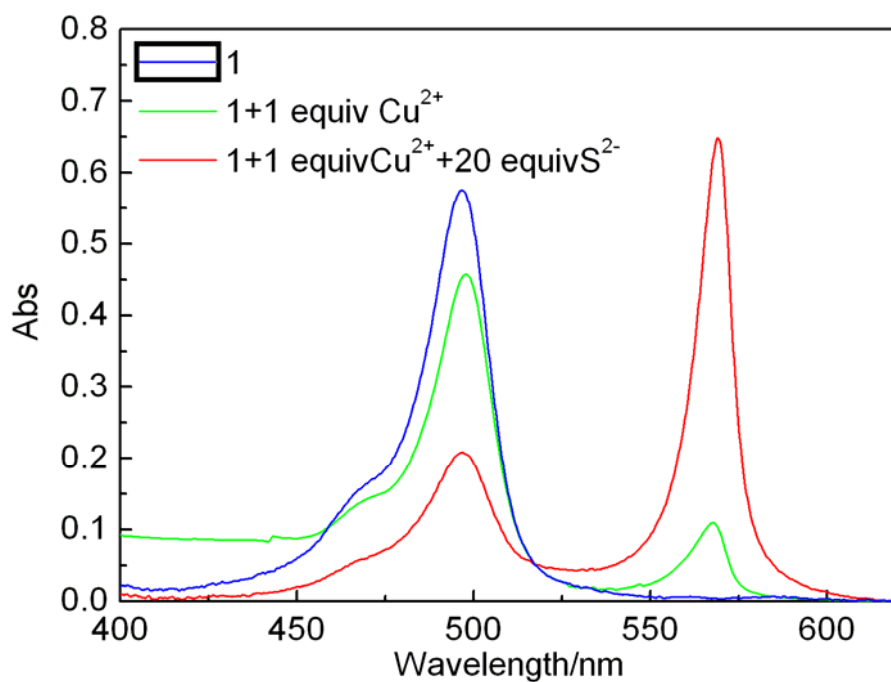


Fig. S3 The absorption spectra of **1** (10 μM) in the presence of 1 equiv of Cu^{2+} and 20 eq of Na_2S .

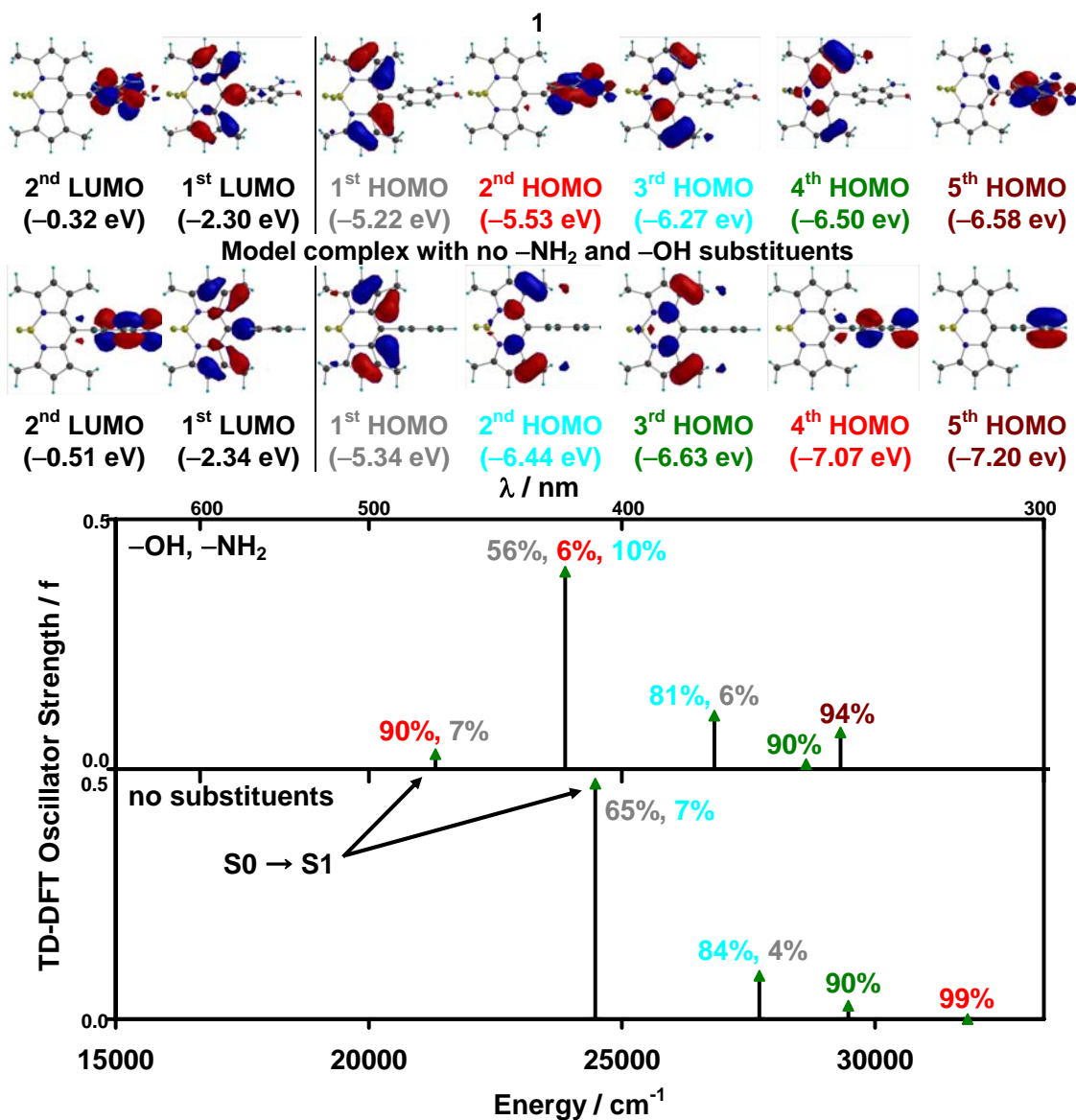


Fig. S4 Frontier π -MOs (TOP) and TD-DFT spectra (BOTTOM) of **1** and a model complex with an unsubstituted phenyl group at an isosurface value of 0.04 a.u. based on a DFT geometry optimisation using the B3LYP functional with 6-31G(d) basis sets. The percentage contribution of one-electron transitions from the first five HOMOs into the 1st LUMO to the bands predicted in the 300 – 600 nm region is colour coded. The S1 state of **1** is predicted to arise primarily from a 2nd HOMO \rightarrow 1st LUMO transition (associated with an occupied MO located primarily on the phenyl substituent), while in the absence of substituents the dominant contribution is the standard 1st HOMO \rightarrow 1st LUMO transition of the BODIPY moiety.

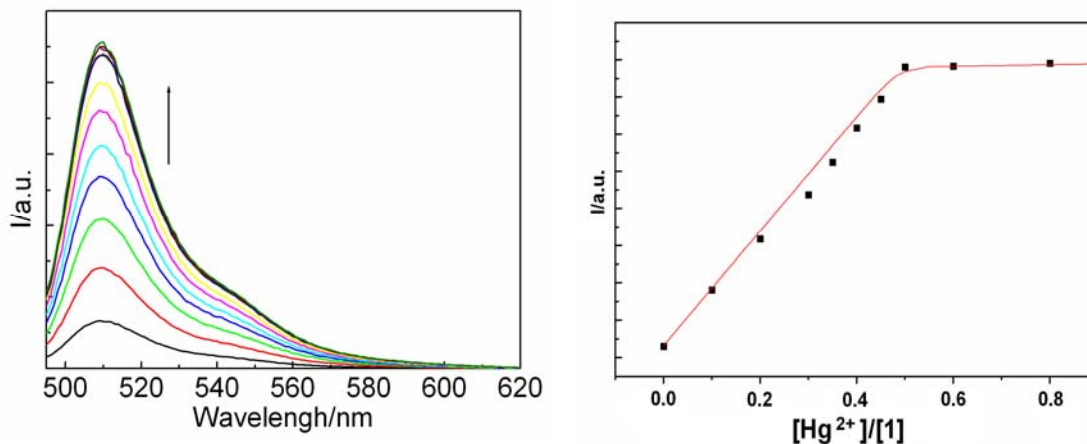


Fig. S5 Fluorescence spectra ($\lambda_{\text{ex}} = 483 \text{ nm}$) of $5 \mu\text{M}$ **1** recorded after the addition of 0, 0.1, 0.2, 0.25, 0.3, 0.35, 0.4, 0.45, 0.5, 0.6, 0.8, 1.0 and 1.2 eq of Hg^{2+} (LEFT). Variations of the $[\text{Hg}^{2+}]/[\mathbf{1}]$ ratio as a function of the fluorescence intensity at 510 nm, the red line corresponds to the best fit with eq (1) (RIGHT).

$$x = \frac{F - F_0}{2(F_{\text{Lim}} - F_0)} \left\{ \frac{1}{K_S} \left[\frac{F_{\text{Lim}} - F_0}{C_0(F_{\text{Lim}} - F)} \right]^2 + 1 \right\} \quad (1)$$

where $x = [\text{Hg}^{2+}]/[\mathbf{1}]$, F is the fluorescence intensity, F_0 and C_0 are the initial fluorescence intensity and concentration of **1**, respectively, F_{Lim} is the limiting fluorescence intensity value upon full complexation and K_S is the stability constant.^{S5}

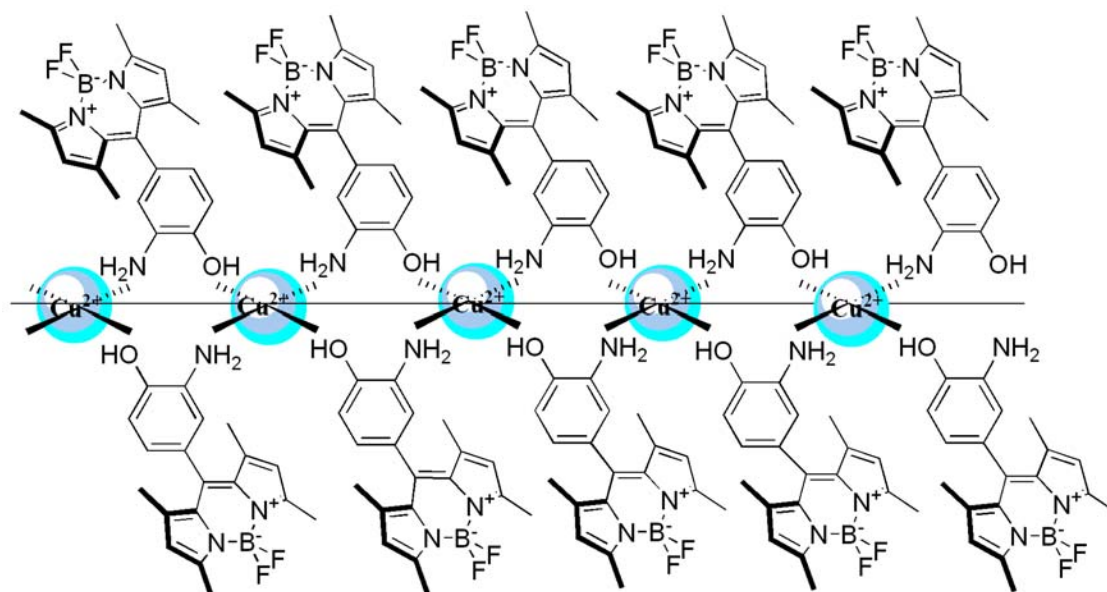


Fig. S6 Model diagram for Cu^{2+} -induced J-aggregation of BDP. The square planar coordination environment typically adopted by Cu^{2+} ions due to their d^9 configuration can facilitate the formation of a regular structure containing parallel BODIPY π -system transition moments.

III. References

- S1 J. Olmsted III, *J Phys Chem.* 1979, **83**, 2581.
- S2 H. Lu, L. Xiong, H. Liu, M. Yu, Z. Shen, F. Li and X. You, *Org. Biomol. Chem.* 2009, **7**, 2554.
- S3 SMART, SAINT, SADABS and SHELXTL, Bruker AXS Inc., Madison, WI, USA, 2000.
- S4 M. J. Frisch, G. W. Trucks, H. B. Schlegel, G. E. Scuseria, M. A. Robb, J. R. Cheeseman, J. A. Montgomery, J. T. Vreven, K. N. Kudin, J. C. Burant, J. M. Millam, S. S. Iyengar, J. Tomasi, V. Barone, B. Mennucci, M. Cossi, G. Scalmani, N. Rega, G. A. Petersson, H. Nakatsuji, M. Hada, M. Ehara, K. Toyota, R. Fukuda, J. Hasegawa, M. Ishida, T. Nakajima, Y. Honda, O. Kitao, H. Nakai, M. Klene, X. Li, J. E. Knox, H. P. Hratchian, J. B. Cross, C. Adamo, J. Jaramillo, R. Gomperts, R. E. Stratmann, O. Yazyev, A. J. Austin, R. Cammi, C. Pomelli, J. W. Ochterski, P. Y. Ayala, K. Morokuma, G. A. Voth, P. Salvador, J. J. Dannenberg, V. G. Zakrzewski, S. Dapprich, A. D. Daniels, M. C. Strain, O. Farkas, D. K. Malick, A. D. Rabuck, K. Raghavachari, J. B. Foresman, J. V. Ortiz, Q. Cui, A. G. Baboul, S. Clifford, J. Cioslowski, B. B. Stefanov, G. Liu, A. Liashenko, P. Piskorz, I. Komaromi, R. L. Martin, D. J. Fox, T. Keith, M. A. Al-Laham, C. Y. Peng, A. Nanayakkara, M. Challacombe, P. M. W. Gill, B. Johnson, W. Chen, M. W. Wong, C. Gonzalez and J. A. Pople, Gaussian 03, Gaussian, Inc., Wallingford CT, 2004.
- S5 (a) J. Bourson, J. Pouget and B. Valeur, *J. Phys. Chem.*, 1993, **97**, 4552; (b) M. N. Berberan-Santos, P. Choppinet, A. Fedorov, L. Jullien and B. Valeur, *J. Am. Chem. Soc.*, 2000, **122**, 11876.

IV. ^1H NMR spectra